

# Surface Tension from Finite-Volume Vacuum Tunneling in the 3D Ising Model

Hildegard Meyer-Ortmanns<sup>1,2</sup> and Thomas Trappenberg<sup>1,3</sup>

*Received*

---

We measure the surface tension  $\sigma$  in the broken phase of the 3D Ising model at a temperature  $T = 0.955T_c$  with two different methods which are taken from quantum field theory in finite volumes. Both methods rely on finite-size effects close to the phase transition. The first one measures  $\sigma$  from the size dependence of the vacuum tunneling energy, which is determined by the decay of a correlation, giving  $\sigma = 0.030$ . The second one extracts  $\sigma$  from the size dependence of the rate of flip events and its corresponding correlation time. It leads to  $\sigma = 0.027$ . Both values agree reasonably with other calculations.

---

**KEY WORDS:** Finite; size analysis; spectrum calculations; field theoretical framework; Ising model; surface tension.

## 1. INTRODUCTION

A careful analysis of finite-size effects was recently made in the four-dimensional Ising model in the context of particle physics.<sup>(1,2)</sup> Beside its role as a toy model for testing numerical and analytical methods, this Ising model is considered in the context of the Salam–Weinberg theory of electroweak interactions. It is the ( $\lambda = \infty$ ) limit of the one-component  $\phi^4$  theory, where  $\lambda$  is the bare scalar coupling constant. The  $\phi^4$  theory is an analogue to the scalar sector of the Salam–Weinberg theory in the sense that the scalar sector is thought to be well approximated by a four-component  $\phi^4$  theory with a lattice cutoff  $\Lambda = a^{-1}$ ,  $a$  being the lattice constant. The  $\phi^4$  theory was investigated by perturbative as well as nonperturbative analytical methods in refs. 3 and 4. Results from high-temperature expansions were used as input to determine the flow of the renormalized scalar self-coupling

---

<sup>1</sup> HLRZ c/o KFA Jülich, P. O. Box 1913, D-5170 Jülich, Federal Republic of Germany.

<sup>2</sup> Institut für Theoretische Physik, Universität Zürich, CH-8001 Zürich, Switzerland.

<sup>3</sup> Institut für Theoretische Physik, RWTH Aachen, D-5100 Aachen, Federal Republic of Germany.

$g_R$  and the renormalized mass  $m_R$  as functions of  $\lambda$  and the hopping parameter  $\kappa$ . It was one of the main purposes of ref. 2 to check the analytical results of ref. 4 in the Ising limit by means of Monte Carlo measurements of  $g_R$  and  $m_R$ . To assure the reliability of the Monte Carlo results, it was important to separate the finite-size effects and trace back their different origin.

One type of finite-size effect which occurs in both phases of the 4D Ising model is due to the field-theoretic vacuum polarization in a finite volume. A second type, the one we will also concentrate on in this paper, is specific for the broken phase. It can be described as a transition between the two degenerate minima of the effective potential and is observed in finite volumes close to the phase transition. In the language of quantum field theory, it is a tunneling between two ground states, or vacua of the system. This "vacuum tunneling" leads to flips of the sign of spin averages and drives the expectation value of the magnetization to zero when a sufficiently large number of Monte Carlo sweeps is made.

Masses and energies of particles correspond to excitations of the ground state in the infinite-volume limit, which is twice degenerated in the broken phase of the Ising model. They are inverses of different bulk correlation lengths  $\xi_b$ . However, in a finite volume, due to tunneling phenomena, the degeneracy of these states is lifted in the Ising model; the spectrum consists of states which are even or odd with respect to the simultaneous flip of signs of all spins. In order to interpret the energies obtained by Monte Carlo simulations in a finite volume as the masses of (multi) particle states, it was ensured in ref. 2 by a suitable choice of parameters that this finite-volume energy splitting of the spectrum is already negligibly small, so that the results for the masses are reliable.

In this paper we consider the Ising model in three dimensions. Concerning the methods, we proceed along the same lines as in refs. 1, 2, doing so, however, in a different spirit. Having in mind that tunneling events correspond to the creation of interfaces in finite boxes, we concentrate on a parameter range (i.e., on an interval of temperature  $T$ ) in the broken phase where tunneling dominates the finite-volume effects. Then we use a finite-size analysis to extract the surface tension  $\sigma$ . The results agree reasonably well with other Monte Carlo estimates.<sup>(5,6)</sup> We also determine some higher excitations of the spectrum. Our methods should be applied when one is limited to lattices of small or intermediate size (limited in view of reasonable computer times). On large enough lattices where finite-size effects are strongly suppressed other methods may be superior to ours (see, e.g., ref. 5).

In Sections 2.1 and 2.3 we outline two methods, later to be called the *static* and the *dynamical* methods, respectively, which we use to calculate

the surface tension. Roughly speaking, in the static method we count flips of “magnetization” in space, i.e., we measure the average length  $\xi_L$  of magnetization domains in configurations. We choose an  $L^2 \times L_z$  “cylinder” geometry with  $L_z \gg L$ , where interfaces build up preferably perpendicular to the cylinder axis. The quantity which determines  $\sigma$  here will be the vacuum tunneling energy  $E_{0a}$ . In the dynamical method we count flips of the total “magnetization” in time, i.e., we count flips occurring during the MC simulation (cf. Fig. 1). This time the “magnetization” refers to  $L^3$ -cubic lattices;  $\sigma$  will be related to a correlation time  $\tau_L$ . Since we switch from a global (cluster) to a local (Metropolis) algorithm between the static and the dynamical method, we discuss the choice of the algorithm in Section 2.2. In Section 3 we give details about the numerical simulations and conclude with the results in Section 4.

To make the paper more self-contained in the context of statistical physics, we summarize our methods in some detail, although they were described already in refs. 1 and 2.

## 2. SURFACE TENSION AND HIGHER EXCITATIONS OF THE SPECTRUM

**The Surface Tension.** The surface tension  $\sigma$  can be defined as the difference between the free energy densities of two large boxes with periodic

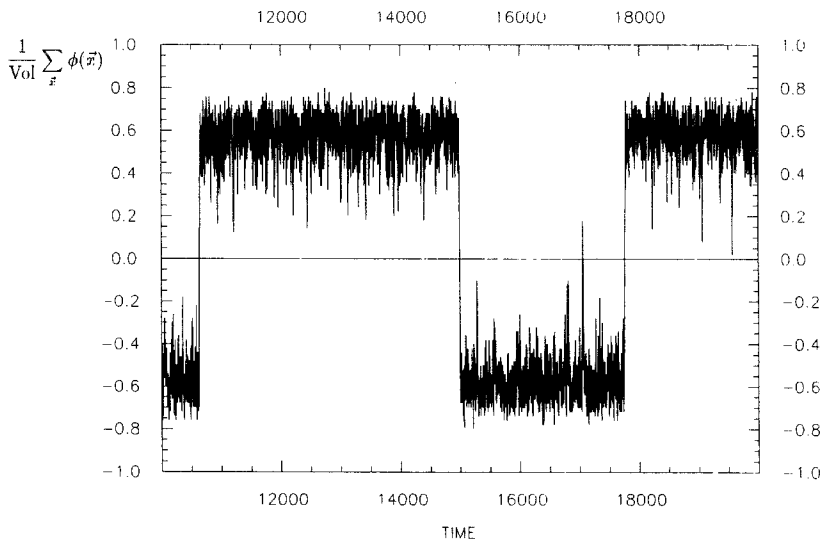


Fig. 1. Flip events of the “magnetization of a given configuration” in time. The time is measured in the number of Monte Carlo iterations. The “magnetization” refers to a cubic box of size  $10 \times 10 \times 10$ .

(p.b.c.) and antiperiodic boundary conditions (a.b.c.), respectively. More precisely, consider a cubic lattice with cylindrical geometry, where the cylinder axis is in the  $z$  direction, and define

$$\sigma := (F_{\text{a.b.c.}} - F_{\text{p.b.c.}})/A \quad (1)$$

where  $A = L^2$  is the cross-section area spanned in the  $x, y$  directions. Here  $F_{\text{a.b.c.}}$  denotes the free energy of the box with a.b.c. in the  $z$  direction and p.b.c. in the  $x, y$  directions.  $F_{\text{p.b.c.}}$  is the free energy of the box with p.b.c. in all directions. Throughout this paper  $\sigma$  should always be understood in units of  $kT$ .

The first way we will extract  $\sigma$  from Monte Carlo simulations is based on the following relation:  $\sigma$  as defined in (1) controls the  $L$  dependence of a certain correlation length  $\xi_L$ ,<sup>(7)</sup> where  $L$  is the linear extension of the cross-section area.  $\xi_L$  is the inverse of the vacuum energy splitting  $E_{0a}$  in the broken phase; asymptotically the  $z$ -slice spin correlation decays as  $\exp(-z/\xi_L)$  in the  $z$  direction.  $E_{0a}$  determines the tunneling amplitudes between the states  $|+\rangle$  and  $|-\rangle$  (which become the degenerate ground states in the infinite-volume limit). The relation between  $\xi_L$  and  $\sigma$  which we use to determine  $\sigma$  is given by

$$E_{0a}^{-1} \equiv \xi_L = C(T)e^{L^2\sigma(T)} \quad (2)$$

Equation (2) was obtained within a semiclassical approximation in ref. 8. The missing  $L$  dependence of the prefactor  $C(T)$  in  $d=3$  was taken as an Ansatz in ref. 8, and we will use it, too, when we determine  $\sigma$  from (2). The  $L$  dependence of  $\sigma$  itself is expected to be exponentially suppressed for large  $L$  (cf. ref. 9 for the case of four dimensions); therefore, we will neglect it here.

Before we go into details about the measurement of  $E_{0a}$ , we summarize the second (so-called dynamical) method, from which we have extracted  $\sigma$  in an alternative way. Yet another correlation, the correlation time  $\tau_L$  in the MC updating of the system, is determined by the surface tension. Using an approach based on the Langevin equation, it was shown in ref. 10 that for Ising-like systems  $\sigma$  is related to  $\tau_L$  according to

$$\tau_L \propto e^{2\sigma(T)L^2} \quad (3)$$

In our dynamical method (see Section 2.3 for detailed definitions), we have counted so-called flip events, where the inverse of the flip rate  $f_M$  defines a correlation time  $\tau_{fM}$ . We will show that  $\tau_{fM}$  is proportional to  $\tau_L$  to a good approximation within the Metropolis algorithm, such that the counting of flip events can serve as a measurement of  $\sigma$  via (3). The factor 2 in (3) can be made plausible from the need for at least two interfaces to allow the average spin to flip.

### 2.1. The Vacuum Tunneling Energy and Higher Excitations of the Spectrum

We consider the three-dimensional Ising model on a cubic lattice with linear extensions  $L_x$ ,  $L_y$ , and  $L_z$ . For the static method we choose  $L_x = L_y = L$  and  $L_z \gg L$  to impose a cylindrical geometry. The action is given by

$$S = -2\kappa \sum_{\mathbf{x}=(x,y,z)} \sum_{\mu=1}^3 \phi_{\mathbf{x}} \phi_{\mathbf{x}+\hat{\mu}} \quad (4)$$

The sums run over pairs of nearest neighbors  $(\mathbf{x}, \mathbf{x} + \hat{\mu})$ , where  $\mu$  denotes the direction of links. Here  $\phi \in \{\pm 1\}$ ,  $\kappa$  is the hopping parameter, which is related to the temperature  $T$  by

$$2\kappa = \frac{J}{kT} \quad (5)$$

where  $J$  denotes the standard coupling constant, and  $k$  is the Boltzmann constant. So the symmetry-breaking transition occurs at  $\kappa = \kappa_c = 0.110827\dots$ . We will choose  $\kappa$  close to  $\kappa_c$  such that we are in the broken phase below the roughening transition at  $\kappa_R = 0.205$ .

To fix our notation, we express the partition function through the transfer matrix in the  $z$  direction,

$$Z = \text{tr} e^{-HL_z} = 1 + e^{-E_{0a}L_z} + e^{-E_{1s}L_z} + e^{-E_{1a}L_z} + e^{-E_{2s}L_z} + \dots \quad (6)$$

The spectrum splits up into even ( $s$ ) and odd ( $a$ ) eigenvalues  $E_{nj}$ ,  $n=0, 1, 2, \dots, j=s, a$ . The corresponding states are denoted by  $|n_s\rangle$  and  $|n_a\rangle$ ,  $n=0, 1, 2, \dots$ . For example, the first excited state  $|0_a\rangle$  in terms of the infinite-volume ground states  $|+\rangle$  and  $|-\rangle$  is given by

$$|0_a\rangle = \frac{1}{\sqrt{2}} (|+\rangle - |-\rangle) \quad (7)$$

corresponding to an energy level  $E_{0a}$ . The energy determines the vacuum tunneling amplitude. It gives the vacuum energy splitting between the degenerate ground states in the broken phase of the finite volume, when the ground-state energy  $E_{0s}$  is normalized to zero. When the energy splitting also for the higher energy levels approaches zero for large enough volumes, we interpret  $E_{ns}$  and  $E_{na}$  as  $n$ -particle thresholds within the context of particle physics.<sup>(1,2)</sup>

We extract the energies  $E_{nj}$  from decays of correlation functions, which are constructed in the following way. Denote a  $z$ -slice spin average by  $S(z)$ ,

$$S(z) \equiv \frac{1}{L^2} \sum_{x,y} \phi(x, y, z) \quad (8)$$

Then the  $z$ -slice correlation of  $S$  in the transfer matrix representation is given by

$$\begin{aligned} \langle S(0) S(z) \rangle &\equiv [\text{Tr}[S(0) e^{-zH} S(z) e^{-(L_z-z)H}]]/Z \\ &= [|\langle 0_s | S(z) | 0_a \rangle|^2 (e^{-E_{0a}z} + e^{-E_{0a}(L_z-z)}) \\ &\quad + |\langle 0_s | S(z) | 1_a \rangle|^2 (e^{-E_{1a}z} + e^{-E_{1a}(L_z-z)}) \\ &\quad + \mathcal{O}(e^{-E_{1s}z}, e^{-E_{1s}(L_z-z)})]/Z \end{aligned} \quad (9)$$

A similar expression can be derived for the connected two-point function of squared spin averages

$$\langle S^2(0) S^2(z) \rangle_c \equiv \langle S^2(0) S^2(z) \rangle - \langle S^2(0) \rangle^2 \quad (10)$$

which we have expanded including terms of  $\mathcal{O}(e^{-E_{2s}z})$ . The energies  $E_{nj}$  can be obtained from (9) and (10) in several ways. The first possibility, which we have only used for consistency checks, we explain with an example. To get a constant  $m$  out of a one-exponential Ansatz (corrected by an exponential function due to the p.b.c.)

$$\Gamma(z) = \text{const} \cdot (e^{-mz} + e^{-m(L_z-z)}) \quad (11)$$

consider ratios of  $\Gamma$  for suitable values of  $z$ , such that it can be solved for  $m$ . In our example  $\Gamma(z=L_z/3)/\Gamma(z=L_z/2)$  would be a good choice. The values for  $E_{nj}$  derived in this way we later call effective energies. They will be used to calculate the statistical errors by means of the binning method which will be briefly discussed below.

Another possibility is to consider  $\langle S(0) S(z) \rangle$  and  $\langle S^2(0) S^2(z) \rangle_c$  as a function of  $z$  and extract  $E_{nj}$  from a fit. We used the following Ansätze for the two-exponential fits:

$$\begin{aligned} \langle S(0) S(z) \rangle &= c_1(e^{-a_0z} + e^{-a_0(L_z-z)}) \\ &\quad + c_2(e^{-a_1z} + e^{-a_1(L_z-z)}) \end{aligned} \quad (12)$$

$$\begin{aligned} \langle S^2(0) S^2(z) \rangle_c &= c_3 + c_4(e^{-s_1z} + e^{-s_1(L_z-z)}) \\ &\quad + c_5(e^{-s_2z} + e^{-s_2(L_z-z)}) \end{aligned} \quad (13)$$

where the constants  $c_1, \dots, c_5$ ,  $a_0$ ,  $a_1$ ,  $s_1$ , and  $s_2$  were determined in the fits. Then they were related to the energies and matrix elements of the transfer matrix representation.

This way of proceeding is more reliable than the first one, when we are able to follow the decay of the correlations over a long distance. To do so, the signal-to-noise ratio has to be optimized. Therefore we chose the

Swendsen–Wang cluster algorithm<sup>(11)</sup> and replaced the spin variables  $\phi(\mathbf{x})$  entering the representation of  $\langle \dots \rangle$  by cluster variables  $n_{c_i}$ . To explain what we mean by that, we spend a few lines on the algorithm.

## 2.2. Choice of the Algorithm

As a nonlocal upgrading procedure we chose the Swendsen–Wang cluster algorithm. It proceeds in the following steps. To a given spin configuration  $\{\phi_{\mathbf{x}}\}_1$  a bond configuration  $\{K_{x_\mu}\}$  is associated, where parallel neighboring spins are connected by a bond according to a probability  $(1 - e^{-4\kappa})$ . Clusters  $c_i$  are sets of neighbors which are connected by bonds. A cluster configuration  $\{n_{c_i}\}$  can be characterized by the number of sites  $n_{c_i}$  belonging to the cluster  $c$  with label  $i$ . The next step in the algorithm is to flip all spins of a cluster with probability 1/2 to obtain in this way the next spin configuration  $\{\phi_{\mathbf{x}}\}_2$ . Our external magnetic field is zero.

We have expressed our correlations  $\langle S(0)S(z) \rangle$  and  $\langle S^2(0)S^2(z) \rangle_c$  in terms of cluster variables  $n_{c_i}(z)$ , where  $n_{c_i}(z)$  denotes the number of sites belonging to the cluster  $c_i$ , here restricted to a  $z = \text{const}$  slice. For further details we refer to ref. 2.

Recall that on the way to equilibrium the Swendsen–Wang algorithm strongly influences the physics of tunneling phenomena, when it enforces flips of large clusters of spins. Therefore, when we are interested in measuring rates of sign flips of certain magnetizations in the finite volume (as we are going to describe in the next section), we might be forced to go back to the local algorithm to get a nontrivial result.

## 2.3. The Dynamical Method, Flip Rates of Average Spins

As in ref. 2, we define the flip rate of average spins in the following way. The “average spin”  $M$  is defined as

$$M(t_k) := \frac{1}{t_k} \sum_{t \in \text{Bin}(t_k)} \frac{1}{\text{Vol}} \sum_{\mathbf{x}=(x,y,z)} \phi^{(t)}(\mathbf{x}) \quad (14)$$

where  $t$  labels the configurations belonging to a bin  $k$  of length  $t_k$  in time. We avoid calling this quantity “magnetization,” since it should not be confused with the magnetization in the infinite-volume limit. For a possible definition of “magnetization” in a finite volume we refer to ref. 1. The flip rate  $f_M$  is defined as the number of flip events in time, where “time” is measured in the number of iterations,

$$f_M := \frac{\# \text{ flip events}}{\# \text{ iterations}} \quad (15)$$

We have normalized  $f_M$  to 100,000 iterations. To indicate the dependence on the algorithm, we use the index  $M$ , where  $M$  stands for ‘‘Metropolis.’’ Finally, a flip event is a change in the sign of  $M(t_k)$ .

There is an ambiguity in the decision of which changes of sign of  $M(t_k)$  should be interpreted as the tunneling events in which we are interested. However, as was observed in refs. 2 and 12, for a certain range of bin lengths  $t_k$  the values for  $f_M$  are quite independent of  $t_k$ , forming a plateau. We interpret the value of  $f_M$  at the plateau as the flip rate. The correlation time  $\tau_{f_M}$  defined as  $f_M^{-1}$  is proportional to the relaxation time  $\tau_L$ , given by (3). Therefore we measured the surface tension in the dynamical method according to

$$\sigma_d = \frac{1}{2} \frac{1}{(L_1^2 - L_2^2)} \ln \frac{(f_M)_2}{(f_M)_1} \quad (16)$$

To get reasonable rates of flip events in time, we used a cubic  $L^3$  geometry for the lattice;  $L_1$  and  $L_2$  denote the linear extensions of different lattice volumes.

To point out that the proportionality between  $\tau_{f_M}$  and  $\tau_L$  depends on the choice of the algorithm, we also defined tentatively an average spin for the Swendsen–Wang algorithm. Let  $n_{\max}$  denote the number of sites in the maximal cluster  $c_{\max}$ ,  $\phi(c_{\max})$  being a representative spin of that cluster. Then an ‘‘average spin’’  $\tilde{M}$  can be defined as

$$\tilde{M} := \frac{1}{t_k} \sum_{t \in \{\text{Bin}(t_k)\}} \left[ \frac{n_{\max}}{\text{Vol}} \text{sgn } \phi(c_{\max}) \right]^{\{t\}} \quad (17)$$

The notation is the same as in (14). Again  $f_c$  is defined as the number of flips in the sign of  $\tilde{M}$  during 100,000 iterations. Using a Swendsen–Wang algorithm, the counting of flip events according to this definition would just provide a test on the random number generator. When we used the same definition for  $\tilde{M}$ , but changed the algorithm in the sense of ref. 13, i.e., keeping the spin orientation of the maximal cluster and choosing the spin orientation of the remaining clusters again à la Swendsen and Wang with probability 1/2, then the flip rate still seemed to obey an exponential law, but the value of  $\sigma$  disagreed by 30% with our value for  $\sigma_d$  and should not be taken seriously. Such a result is not surprising, since the dynamics which determines the approach to equilibrium depends on the algorithm and might interact with finite-size phenomena.

### 3. NUMERICAL SIMULATIONS

**Choice of the Temperature.** After a series of short runs we found a value of  $\kappa$  ( $\kappa = 0.116$ , corresponding to  $T = 0.955T_c$ ) which was



suitable in the sense that both of our methods were applicable within reasonable computer times. If  $\kappa$  is too large, i.e., if we are deeply in the broken phase, the tunneling events are rare, the signal of the tunneling energy  $E_{0a}$  is of the order of the statistical noise, and the energy splitting  $E_{1a} - E_{1s}$  shrinks to zero. On the other hand, if  $\kappa$  is too close to the critical point, i.e., the bulk correlation length  $\xi_b$  is no longer small compared to the lattice size ( $\xi_b \ll L$  would be desirable), finite-size effects due to the periodicity of the lattice will be strong, which are not specific for the broken phase. Also, the equilibration of the sample would suffer from critical slowing down.

**Simulations in the Static Method.** The simulations for the static method using the cluster algorithm were made on cylindrical lattices of size  $L^2 \times 120$ , where  $L$  varied from 8 to 14. After discarding the first 1000 sweeps for equilibration, we made 200,000 sweeps per site.

We have measured the correlations  $\langle S_0 S_z \rangle$  and  $\langle S_0^2 S_z^2 \rangle_c$  up to distances 60.  $E_{0a}$  and  $E_{1a}$  were determined from a two-exponential fit of  $\langle S_0 S_z \rangle$  according to (12);  $a_0$  and  $a_1$  were identified with  $E_{0a}$  and  $E_{1a}$ , respectively. In Fig. 2 an example is shown for  $L = 10$ . To our surprise we had to use a two-exponential fit also for  $\langle S_0^2 S_z^2 \rangle_c$ , cf. (13), where  $s_1, s_2$  were identified with  $E_{1s}, E_{2s}$ , respectively. (In the four-dimensional Ising model the  $E_{2s}$  excitation did not show up in comparable runs.<sup>(2)</sup>)

Since now we are mainly interested in extracting the surface tension, we list the values for  $E_{0a}$  obtained from the fits for several values of  $L$  in the second column of Table I; cf. also Fig. 3.

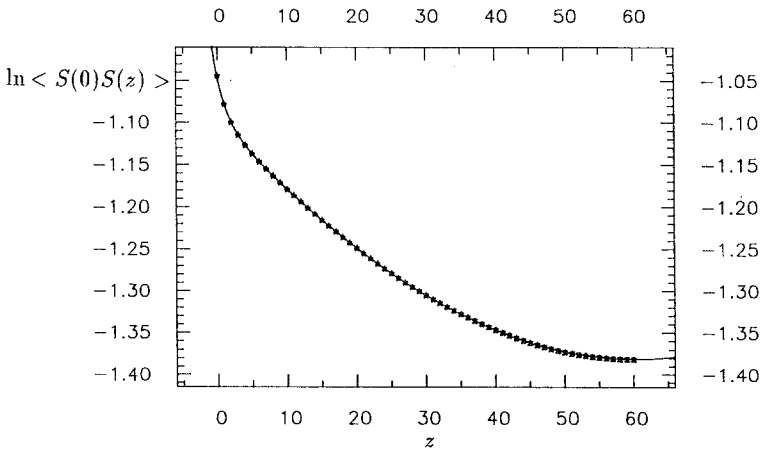


Fig. 2. Two-exponential fit of the  $z$ -slice correlation  $\langle S_0 S_z \rangle$  for 60 values of the  $z$ -slice distance  $z$ . The exponents give  $E_{0a}$ , the tunneling energy, and  $E_{1a}$ , the higher excitation. The  $z = 0$  value of  $\langle S_0 S_z \rangle$  was excluded for the fit.

**Table I. Tunneling Energies  $E_{0a}$  and Number of Flip Events  $f_M$  and  $f_c$  Normalized to  $10^5$  Iterations in the Metropolis and the Modified Cluster Algorithm for Several Choices of Linear Extensions  $L$**

$L$	$E_{0a}$	$f_M$	$f_c$
8	0.0393(1)	—	360(30)
10	0.01316(8)	28.7(6)	96(5)
12	0.00345(7)	2.6(2)	16(2)
14	0.00080(6)	0.16(1)	—

The indicated purely statistical errors in the last digits were obtained in the following way. The total number of configurations was subdivided into bins of length  $2^n$  ( $n \in \mathbb{N}$ ). For a given observable and a given bin length, the errors of bin averages were calculated in the standard way. When it happens that the error becomes independent of the bin length for some range of bin lengths, it is taken as the statistical error of the observable. In this way we got a statistical error of the correlations, which enter the fit for  $E_{0a}$ , and for the effective energies  $E_{0a}$ ,  $E_{1s}$ ,  $E_{1a}$ , which were calculated as indicated above. The errors of the values for  $E_{0a}$  in Table I

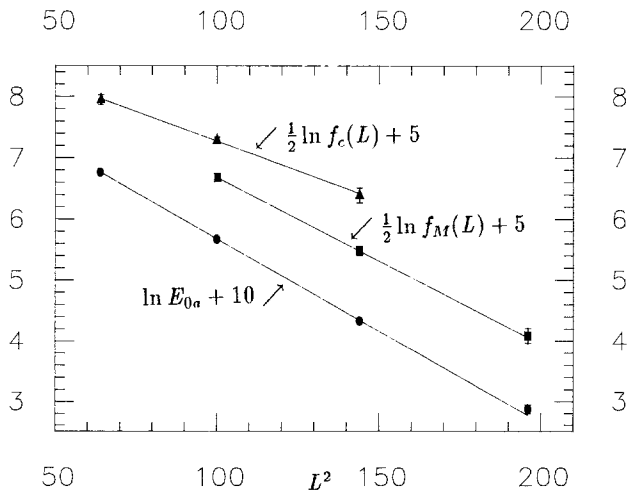


Fig. 3. The  $L$  dependence of the tunneling energy  $E_{0a}$  and the flip event rates  $f_M$  and  $f_c$ . On the ordinate we have plotted  $\ln E_{0a} + 10$ ,  $\frac{1}{2} \ln f_M + 5$ , and  $\frac{1}{2} \ln f_c + 5$ . The slope of the curves for  $\ln E_{0a}$  and  $\frac{1}{2} \ln f_M$  yields  $\sigma_s$  and  $\sigma_d$ , respectively. The slope of  $\frac{1}{2} \ln f_c + 5$  differs significantly from the others. It would lead to a value for  $\bar{\sigma}$  of 0.019.

are the statistical errors of the effective energies. We have checked for consistency that these errors are compatible with the errors involved in the fit procedure (statistical errors for  $\langle S_0 S_z \rangle$  and dependence on the number of fitted points).

**Simulations in the Dynamical Method.** For this method the simulations were made on cubic lattices of volume  $L^3$  between  $8^3$  and  $14^3$ . Here we discarded the first 10,000 sweeps for equilibration. For the upgrading procedure we used the standard Metropolis algorithm in a vectorized form. To collect enough statistics for the flip rate, we made up to  $5 \times 10^6$  sweeps, depending on  $L$ .

The flip rates  $f_M$  for the Metropolis algorithm from which  $\sigma_d$  was calculated later are shown in column 3 of Table I. In column 4 the rates  $f_c$  within the modified cluster algorithm are displayed, although as a way to find  $\sigma$  they should be disregarded. The errors in  $f_M(f_c)$  as indicated for  $L = 8, 10, 12$  result from the ambiguity in the choice  $t_K$  of bin length, which was taken to be representative to decide whether a sign flip of the average

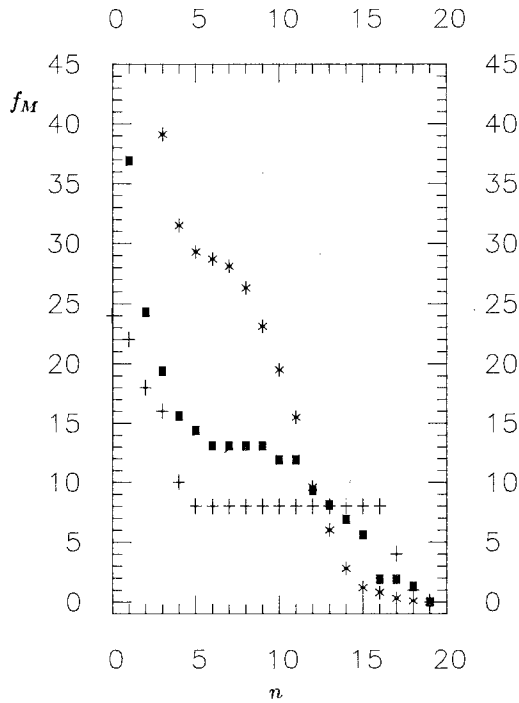


Fig. 4. Flip event rate  $f_M$  as a function of  $n$ , where the bin length  $t_k$  is given by  $t_k = 2^n$  for three different volumes after (+) 5,000,000 sweeps for  $L = 14$ , (■) 500,000 sweeps for  $L = 12$ , (\*) 100,000 sweeps for  $L = 10$ . For smaller volumes the plateau in  $f_M$  is less pronounced.

spin should be considered as a flip event or not. Figure 4 shows that the plateau in  $f(t_k)$  is less pronounced for smaller volumes; therefore, the corresponding errors involved in the choice of  $t_k$  dominated the statistical ones. Conversely, for  $L = 14$  the statistical error of  $\pm 0.01$  for  $f_M$  was larger. It was obtained from five runs of about  $10^6$  sweeps each.

#### 4. RESULTS

**The Surface Tension.** For the surface tension  $\sigma_s$  in units of  $kT$  extracted from the vacuum tunneling energy  $E_{0a}$  within the static method we obtained

$$\sigma_s = 0.0303 \quad (18)$$

The values of  $E_{0a}(L)$  were taken from the fits of the correlations  $\langle S(0)S(z) \rangle$ . Observation of the rate of flip events within the dynamical method led to

$$\sigma_d = 0.0273 \quad (19)$$

The statistical errors for both values are of the order of  $10^{-4}$ . Therefore  $\sigma_s$  and  $\sigma_d$  do not agree within the statistical errors. We take this as an indication that we are not deeply enough in the asymptotic region of large  $L$ , where the formulas (2) and (3) should hold. The exponent  $\sigma L^2$  was still of the order of 6, which is not very large.

The value of  $\sigma_s$  is 10% lower than the value given by Mon,<sup>(5)</sup> who gets  $\sigma = 0.0328$  extrapolated from  $T \rightarrow T_c$ . It is about 30% larger than the value of Binder<sup>(6)</sup> ( $\sigma = 0.0218$ ).  $\sigma_d$  differs by 20% from Binder's value.

Usually, flip events in the context of particle physics are just considered as disturbing artifacts of the finite volume which should be suppressed. This point of view can be also found in papers of statistical physics.<sup>(14)</sup> As is demonstrated by our results, these "artifacts" contain valuable information on physical quantities when they are analyzed with respect to their finite-size scaling behavior. We find it amazing that the surface tension which also enters universal ratios of binary mixtures can be estimated from counting these flip events from plots like Fig. 1. Nevertheless, we consider the dynamical method more as a heuristic one (due to the ambiguity in what is called a flip event and a possible influence of the algorithm).

**Higher Excitations.** The  $L$  dependence of  $E_{1s}$ ,  $E_{1a}$ , and  $E_{2s}$  (as well as  $E_{0a}$ ) as they were obtained from the two-exponential fits are shown in Fig. 5. As expected,  $E_{0a}$  and  $\Delta E_1 = E_{1s} - E_{1a}$  decrease with increasing  $L$ ;

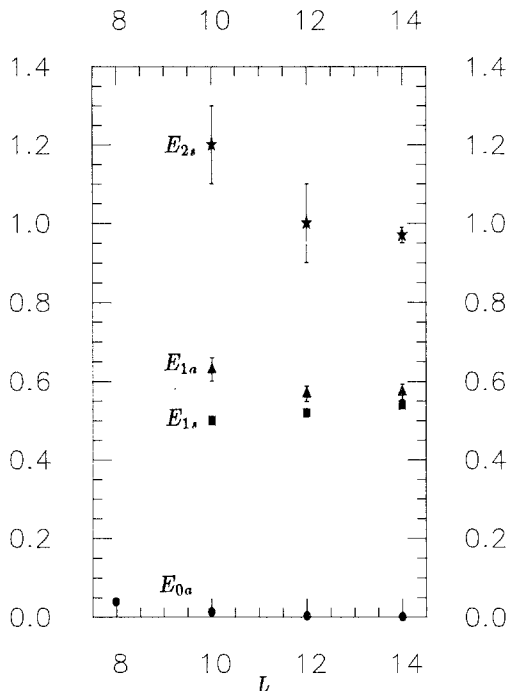


Fig. 5. The  $L$  dependence of the energies  $E_{nj}$  ( $n=0, 1, 2; j=s, a$ ) at  $\kappa=0.116$ . The  $E_{nj}$  are taken from the corresponding  $z$ -slice-correlation fits.

they should vanish in the infinite-volume limit. We remark that  $E_{0a}$  should not be misinterpreted as the one-particle mass in the broken phase, which corresponds to  $E_{1s}$  and  $E_{1a}$  provided  $\Delta E_1 \approx 0$ . Furthermore, for a volume large enough that both  $\Delta E_1$  and  $\Delta E_2$  are almost zero,  $E_{1s} \simeq E_{1a}$  and  $E_{2s} \simeq E_{2a}$  would determine the scattering length of two particles in the broken phase.<sup>(15)</sup>

In the context of statistical physics we speculate that the higher excitations  $E_{1s}$ ,  $E_{1a}$  might be related to the surface stiffness coefficient,<sup>(16)</sup> since our correlations in the  $z$  direction should be sensitive to excitations perpendicular to the interfaces spanned in the  $x, y$  directions of the box.

To estimate the systematic errors involved in both of our methods, it would be useful to try them also in two dimensions where exact results are available.

## ACKNOWLEDGMENTS

We are indebted to D. Stauffer for stimulating discussions. We thank the authors of ref. 2 for supplying us with some of their routines for the algorithms. We are also grateful to J. Jersák for useful comments. H.M.-O. was supported in part by the Schweizerischer Nationalfonds; T. T. was supported by the Deutsche Forschungsgemeinschaft.

## REFERENCES

1. K. Jansen, J. Jersák, I. Montvay, G. Münster, T. Trappenberg, and U. Wolff, *Phys. Lett.* **213B**:203 (1988).
2. K. Jansen, I. Montvay, G. Münster, T. Trappenberg, and U. Wolff, *Nucl. Phys. B* **322**:698 (1989).
3. M. Lüscher and P. Weisz, *Nucl. Phys. B* **290**[FS20]:27 (1987).
4. M. Lüscher and P. Weisz, *Nucl. Phys. B* **295**[FS21]:65 (1988).
5. K. K. Mon, *Phys. Rev. Lett.* **60**:2749 (1988).
6. K. Binder, *Phys. Rev. A* **25**:1699 (1982).
7. M. E. Fisher, *J. Phys. Soc. Japan* (Suppl.) **26**:87 (1969).
8. E. Brézin and J. Zinn-Justin, *Nucl. Phys. B* **257**[FS14]:867 (1985).
9. G. Münster, DESY 89-011 (February 1989); *Nucl. Phys. B*, in press.
10. J. C. Niel and J. Zinn-Justin, *Nucl. Phys. B* **280**[FS18]:355 (1986).
11. R. H. Swendsen and J.-S. Wang, *Phys. Rev. Lett.* **58**:86 (1987).
12. T. Trappenberg, Diploma thesis.
13. Z. Alexandrowitz, *Physica A*, in press.
14. U. Staaden and M. Fähnle, preprint MPI für Metallforschung Stuttgart (1989).
15. M. Lüscher, *Commun. Math. Phys.* **104**:177; **105**:153 (1986).
16. V. Privman and N. M. Švrakić, *J. Stat. Phys.* **54**:735 (1989).